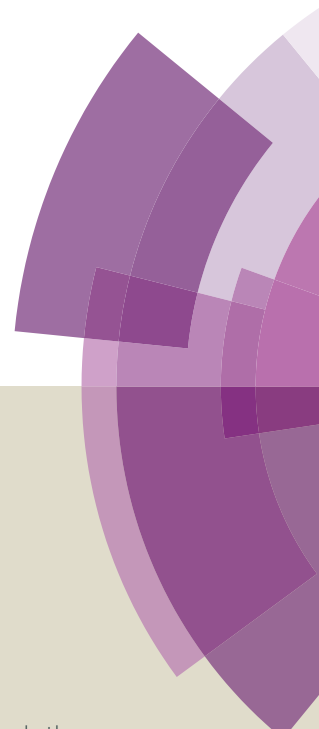


# Journal of Materials Chemistry A

Accepted Manuscript



This article can be cited before page numbers have been issued, to do this please use: N. Wang, W. Chen, W. Shen, L. Duan, M. Qiu, J. Wang, C. Yang, Z. Du and R. Yang, *J. Mater. Chem. A*, 2016, DOI: 10.1039/C6TA03709G.



This is an *Accepted Manuscript*, which has been through the Royal Society of Chemistry peer review process and has been accepted for publication.

*Accepted Manuscripts* are published online shortly after acceptance, before technical editing, formatting and proof reading. Using this free service, authors can make their results available to the community, in citable form, before we publish the edited article. We will replace this *Accepted Manuscript* with the edited and formatted *Advance Article* as soon as it is available.

You can find more information about *Accepted Manuscripts* in the [Information for Authors](#).

Please note that technical editing may introduce minor changes to the text and/or graphics, which may alter content. The journal's standard [Terms & Conditions](#) and the [Ethical guidelines](#) still apply. In no event shall the Royal Society of Chemistry be held responsible for any errors or omissions in this *Accepted Manuscript* or any consequences arising from the use of any information it contains.



## Journal of Materials Chemistry A

## ARTICLE

# Novel Donor–Acceptor Polymer Containing *o*-Fluoro-*p*-alkoxyphenyl-Substituted Benzo[1,2-*b*:4,5-*b'*]dithiophene Unit for Polymer Solar Cells with Power Conversion Efficiency Exceeding 9%

Received 00th January 20xx,  
Accepted 00th January 20xx

DOI: 10.1039/x0xx00000x

www.rsc.org/

Ning Wang,<sup>‡</sup> Weichao Chen,<sup>‡</sup> Wenfei Shen,<sup>a</sup> Linrui Duan,<sup>a</sup> Meng Qiu,<sup>a</sup> Junyi Wang,<sup>a</sup> Chunming Yang,<sup>b\*</sup> Zhengkun Du,<sup>a</sup> Renqiang Yang<sup>a,c\*</sup>

In this work, a new electron-rich building block, *o*-fluoro-*p*-alkoxyphenyl-substituted benzo[1,2-*b*:4,5-*b'*]dithiophene (BDT) unit has been used to construct donor (D)–acceptor (A) conjugated copolymers with electron-deficient units 5,6-difluoro-4,7-di(4-(2-ethylhexyl)-2-thienyl)-2,1,3-benzothiadiazole (C8DTBTff) and 5,6-difluoro-4,7-di(4-hexyl-2-thienyl)-2,1,3-benzothiadiazole (C6DTBTff), named P-*o*-FBTDP-C8DTBTff (P2) and P-*o*-FBTDP-C6DTBTff (P3), respectively. The experimental results indicate that the incorporation of the fluorine onto the *ortho*-position of alkoxyphenyl substituted BDT unit can enable its resultant polymer to efficiently tune the energy levels and improve the mobility of the derived bulk heterojunction layer, which results in much higher power conversion efficiency (PCE) of P2 (8.10%). Moreover, replacing the 2-ethylhexyl chains on the DTBTff unit with hexyl chains can improve the planarity of the conjugated backbone of the polymer, which makes the P3/PC<sub>71</sub>BM blends exhibit higher carrier mobility than P2/PC<sub>71</sub>BM. Finally, a PCE of 9.02% for the device of P3 is obtained without any additive treatment, which is the highest value for the widely reported D-A polymers with fluorine substituted BDT as electron-donor units in single junction polymer solar cells.

## 1. Introduction

Bulk heterojunction polymer solar cells (PSCs) have attracted much attention in the past decade, owing to their flexibility, low fabrication cost, and light weight<sup>1–6</sup>. Recently, PSCs based on conjugated polymers and fullerene derivatives have made significant progress toward commercialization. The power conversion efficiencies (PCEs) over 10% have been obtained for the single junction PSC devices<sup>7,8</sup>.

In the active layer of PSCs, the conjugated polymers with alternating electron-rich units (electron-donor, D) and electron-deficient moieties (electron-acceptor, A), known as D–A copolymers, are one of the most efficient design strategies to obtain high-performance donor materials, since it can offer the unique feature of tuning the energy levels, band

gaps, and mobility through modifying the chemical structure and conformation of D or A moieties<sup>9–13</sup>. Until now, a large amount of donor materials have been designed and synthesized as new D–A copolymer photovoltaic materials. As the electron-rich moiety, BDT has the structure of fusing benzene with two thiophene moieties, which endows it a rigid and planar conjugated structure<sup>14</sup>. The central benzene core of the BDT unit can be substituted by different groups to tune the properties including energy level, band gap, and mobility of the polymers<sup>15</sup>. For example, the conjugated substituted groups with aromatic structure can enhance intermolecular  $\pi$ – $\pi$  interactions, which can be beneficial to improving the photovoltaic properties of conjugated polymers<sup>16–18</sup>. Moreover, it has been proven that introduction of fluorine atom onto the BDT unit can also efficiently influence the photovoltaic performance of D–A polymers due to the strong electron-withdrawing ability of the fluorine atom<sup>19</sup>. Furthermore fluorine substitution can also alter the surface energy of the polymer and thus greatly influence the morphology of the active layer through weak bonds such as C–F...H and F...S interaction<sup>20</sup>. Figure 1 shows the possible substituted positions on alkoxy-, thienyl-, and phenyl-substituted BDT units. The performance of the reported polymers with the above fluorinated BDT units is listed in Table 1. Interestingly, the positions where the fluorine atoms are bonded may result in much difference in the performance of

<sup>a</sup> CAS Key Laboratory of Bio-based Materials, Qingdao Institute of Bioenergy and Bioprocess Technology, Chinese Academy of Sciences, Qingdao 266101, China. E-mail: yangrq@qibebt.ac.cn

<sup>b</sup> Shanghai Synchrotron Radiation Facility, Shanghai Institute of Applied Physics, Chinese Academy of Sciences, Shanghai 201204, China. E-mail: yangchunming@sinap.ac.cn

<sup>c</sup> State Key Laboratory of Luminescent Materials and Devices, South China University of Technology, Guangzhou 510641, China.

†Electronic Supplementary Information (ESI) available: [details of any supplementary information available should be included here]. See DOI: 10.1039/x0xx00000x

‡These authors contributed equally to this work.

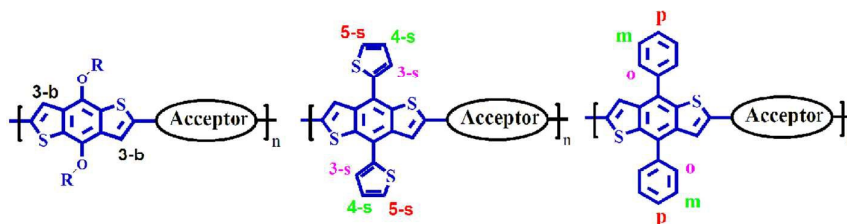


Figure 1. The possible fluorine substituted positions on BDT based donor-acceptor (D-A) polymers.

Table 1. The effect of the F substituted positions on the performance of the BDT based polymers.

polymer	F-position <sup>a</sup>	$V_{oc}$ (V)	$J_{sc}$ (mA cm <sup>-2</sup> )	FF (%) <sup>d</sup>	PCE <sub>max</sub> (%)	$\Delta$ PCE <sup>e</sup>	Ref.
PTBF3	3-b	0.76	9.1	39	2.7	N/A	[21]
PTBF2	3-b	0.75	11.1	42	3.2	0.5	[21]
PBO- <i>p</i> -FPO	<i>p</i>	0.97	9.9	53	5.1 <sup>b</sup>	1.9	[25]
PTFBDT-BZO	<i>m</i> <sup>c</sup>	0.96	9.24	64	5.67	0.6	[26]
PBQ-2	4-s	0.76	13.05	63	6.25	0.58	[22]
PBDTPF-DTBT	<i>m</i>	0.82	13.11	65	7.02	0.77	[24]
PBT-2F	4-s	0.74	14.4	68	7.2	0.2	[23]
PBO- <i>m</i> -FPO	<i>m</i>	0.87	14.3	64	8.0 <sup>b</sup>	0.8	[25]
P2	<i>o</i>	0.94	12.48	69	8.10	0.1	This work
PTFBDT-BZS	<i>m</i> <sup>c</sup>	0.89	12.67	73	8.24	0.14	[26]
PBQ-4	4-s	0.90	13.58	70	8.55	0.31	[22]
PBT-3F	4-s	0.78	15.2	72	8.6	0	[23]
P3	<i>o</i>	0.93	12.97	74	9.02	0.4	This work

<sup>a</sup>The substituted position of fluorine on the BDT moiety with different side chains; <sup>b</sup>The values were obtained from the devices with optimized interfacial layer; <sup>c</sup>Two fluorine atoms were introduced on the *meta*-positions of BDTP segment. <sup>d</sup>The decimal digits in some FF are rounded to the nearest unit. <sup>e</sup>Incremental PCE values compared to the data in the previous row, the decimal digits in some PCE are rounded to the nearest unit before calculation.

the polymers. For example, Yu and coworkers reported that the modification of the thiophene ring (3-b position of BDT units in Figure 1) by fluorination could have a significant effect on the physical properties of polymers<sup>21</sup>, however, PCEs only reached 3.3% and 2.8% for polymer PTBF2 and PTBF3, respectively, which was ascribed to the poor miscibility of the polymers with [6,6]-phenyl-C<sub>71</sub>-butyric acid methyl ester (PC<sub>71</sub>BM) and the lower mobility of the polymers. Hou and coworkers reported the fluorination of the conjugated thienyl- side groups of the BDT unit, and showed synergistic effect on molecular energy level modulation of the polymers. When the quinoxaline derivatives were employed as acceptor unit to construct D-A polymer, a high PCE of 8.55% was obtained for the polymer PBQ-4<sup>22</sup>; while the thieno[3,4-b]thiophene (TT) was selected, a comparative PCE value of 8.6% was achieved for polymer PBT-3F<sup>23</sup>. Compared to thienyl- group, phenyl-group had better symmetric structure and weaker electron-donating ability. As shown in Figure 1, there are three reaction sites on the phenyl substituted BDT (BDTP) moiety including *para*-, *meta*-, and *ortho*-positions. While fluorine atoms are introduced to the above positions, the electron density of the polymer backbone will be redistributed due to the strong electron inductive effects of fluorine, which will further affect the energy levels of the conjugated polymers. Recently, our group introduced fluorine at the *meta*-position of the alkoxyphenyl group substituted BDT unit. The resulting polymer showed a relatively low lying highest occupied molecular orbital (HOMO) energy level, and the device based

on the polymer and PC<sub>71</sub>BM exhibited good photovoltaic performance with PCE of 7.02%, open-circuit voltage ( $V_{oc}$ ) of 0.82 V, short-circuit current density ( $J_{sc}$ ) of 13.11 mA cm<sup>-2</sup> and fill factor (FF) of 65.28%<sup>24</sup>. Meanwhile, Zou et. al. also compared two polymers containing *meta*-fluoro-*para*-alkoxyphenyl- (*m*-FPO-) and *para*-fluoro-*meta*-alkoxyphenyl- (*p*-FPO-) substituted BDT segment, and showed quite different photovoltaic performance of the two polymers<sup>25</sup>. Most recently, Bo et al. introduced two fluorine atoms on the *meta*-positions of the BDT moiety, and reported two polymers with 4-alkyl-3,5-difluorophenyl substituted benzodithiophene as the electron donor moiety, benzothiadiazole or benzooxadiazole as the electron acceptor unit, named PTFBDT-BZS and PTFBDT-BZO, respectively. The photovoltaic devices with PTFBDT-BZS:PC<sub>71</sub>BM as the active layer showed PCE of 8.24% without any additive treatment<sup>26</sup>. As shown in Figure 1, the *ortho*-position is adjacent to the conjugated backbone, where fluorine can influence the molecular packing and photovoltaic performance of the two-dimensional (2D) conjugated polymers efficiently.<sup>27,28</sup>, however, to our best knowledge, there is still no report about the modification on the *ortho*-positions of BDTP.

Based on the above considerations, we introduced fluorine atom to the *ortho*-position of the BDTP unit, and prepared the polymer P-*o*-FBDTP-C8DTBTff (P2) with the well-known electron-withdrawing monomer 5,6-difluoro-4,7-di(4-(2-ethylhexyl)-2-thienyl)-2,1,3-benzothiadiazole (C8DTBTff).

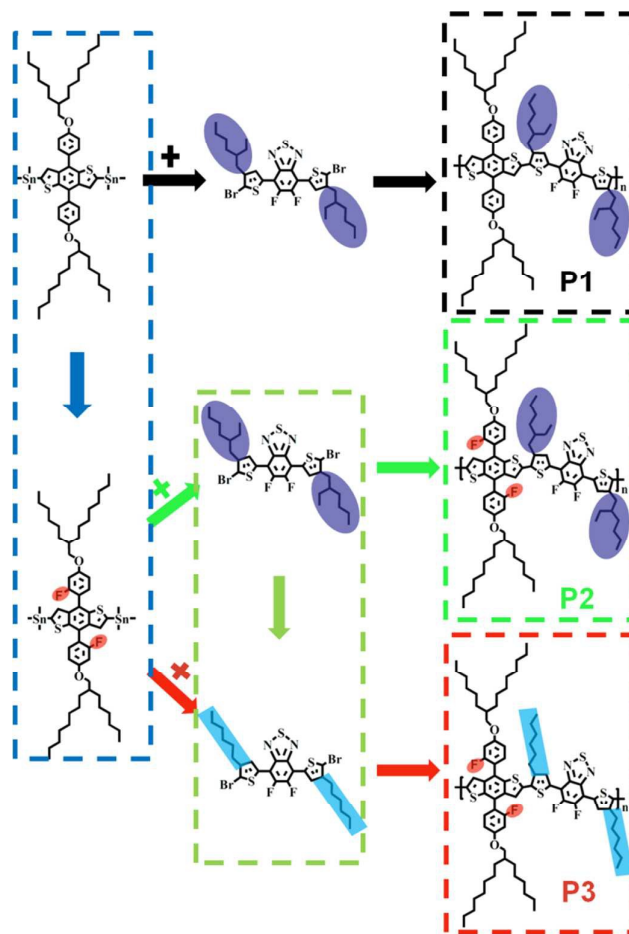


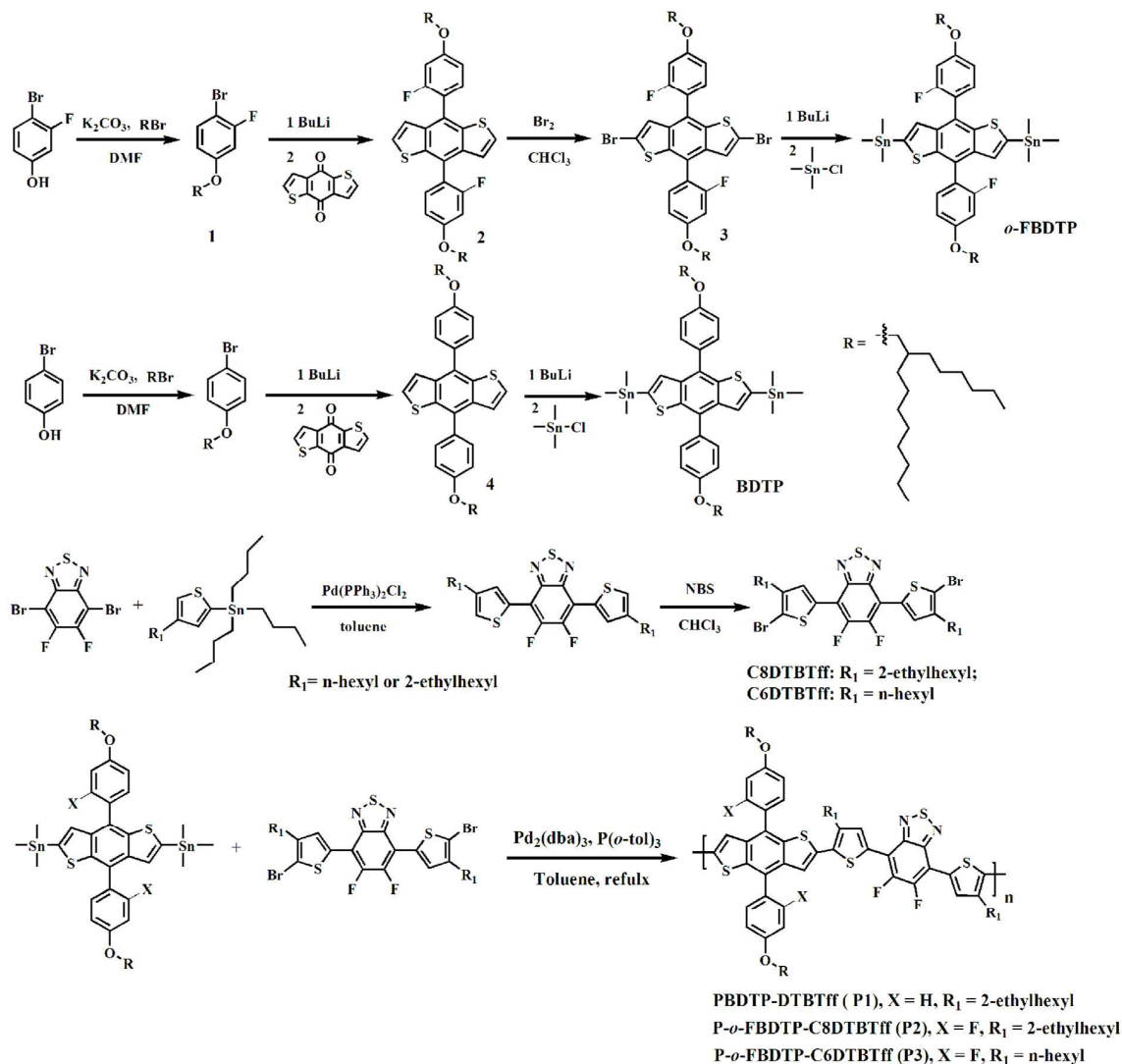
**Figure 2.** The design strategy and structures of copolymers P1, P2, and P3.

Meanwhile, PBDBP-DTBTff (P1) without F on phenyl group was prepared as a reference polymer. The design strategy and structures of polymers are shown in Figure 2. The inclusion of the F atom on the *ortho*-position of alkoxyphenyl substituted BDT unit greatly decreased the HOMO energy level of P2. As a result, the  $V_{oc}$  value was increased to 0.94 V for P2. Meanwhile, the inclusion of the F atom in the conjugated side chain of polymer also increased the mobility and regulated the morphology of the active layer. These synergistic effects increased PCE of P2-based devices to 8.10% after additive treatment. Furthermore, considering the steric effect of the alkyl chain on the thiophene bridge of DTBTff unit<sup>29</sup>, we replaced the 2-ethylhexyl chain in P2 with hexyl chain in the DTBTff moiety, and prepared polymer P3, which showed more planarity backbone than P2. Inspiringly, the mobility of P3/PC<sub>71</sub>BM film gave  $1.5 \times 10^{-4} \text{ cm}^2 \text{ V}^{-1} \text{ s}^{-1}$ , which was about 2.6 times higher than that of P2/PC<sub>71</sub>BM film. Finally, the PSC device based on P3 and PC<sub>71</sub>BM showed the highest PCE of 9.02% with  $V_{oc}$  of 0.93 V, a  $J_{sc}$  of  $12.97 \text{ mA cm}^{-2}$  and a FF of 74.49% (Table 1).

## 2. Results and Discussion

### 2.1. Synthesis and Characterization

The synthetic routes for the monomers and the target polymers are shown in Scheme 1. The alkoxyphenyl or *o*-fluorine alkoxyphenyl substituted groups were bound to BDT via the nucleophilic and reduction reaction to afford compound 4 and 2, respectively<sup>30</sup>. It should be noted that the hydrogen atom on the meta-position of the *o*-fluorine alkoxyphenyl substituted group in compound 2 has high reactivity due to the combined *ortho* directing effects of the adjacent fluoro- and alkoxy-groups<sup>31</sup>. Subsequently, the monomer *o*-FBDBP was prepared from bromated BDT derivative (compound 3) by lithiation using butyl lithium and then quenching with trimethyltin chloride with satisfying yield, which was obviously different from the BDBP with one pot reaction. The electron deficient monomer C8DTBTff<sup>20</sup> and C6DTBTff<sup>32</sup> were synthesized through Stille coupling reaction between 4,7-dibromo-5,6-difluoro-2,1,3-benzothiadiazole and 2-tributylstannyl-4-alkylthiophene, followed by the bromination reaction, respectively.



**Scheme 1.** Synthetic routes of the monomers and polymers.

Finally, the D–A structured polymers were obtained via Stille cross-coupling polycondensation in the presence of  $\text{Pd}_2(\text{dba})_3$  catalyst and tri(*o*-tolyl)phosphine ligand with high yields<sup>33</sup>. All the polymers can be dissolved in common organic solvents such as chloroform, chlorobenzene, and 1,2-dichlorobenzene. The number-average molecular weights ( $M_n$ ) of the polymers were measured by gel permeation chromatography (GPC) (Table S1). There was only small difference in the  $M_n$  and PDI values of the three polymers, which indicated that the photovoltaic performance of these polymers was not mainly influenced by the molecular weights. The thermal properties of the polymers were carried out by the thermogravimetric analysis (TGA). As shown in Fig. S1 and Table S1, all the polymers exhibit good thermal stability and the decomposition temperature ( $T_d$ ) at 5% weight loss is over 330 °C.

## 2.2. Energy levels and Optical Properties

Electronic energy levels of the polymers are crucial for their application in OPVs. To evaluate the molecule energy levels of the synthesized three polymers, their HOMO and lowest unoccupied molecular orbital (LUMO) were measured by both cyclic voltammetry (CV) and ultraviolet photoelectron spectroscopy (UPS) methods. As shown in Figure S2a, the polymer films exhibited an irreversible oxidative potential. The HOMO energy levels of the polymers were estimated from the onset potentials according to the equation  $\text{HOMO} = -[(E_{\text{onset}} - E_{\text{foc}}) + E_{\text{ref}}]$  (eV), where  $E_{\text{foc}}$  is the potential of the external standard, the ferrocene/ferrocenium ion ( $\text{Foc}/\text{Foc}^+$ ) couple, and  $E_{\text{ref}}$  is the reference energy level of ferrocene (4.8 eV below the vacuum level<sup>34</sup>). As shown in Table 2, the HOMO energy levels of P1, P2 and P3 calculated in this method were 5.50, -5.63 and -5.56 eV, respectively. It could be seen from the CV results that the HOMO of P2 was lower than that of P1, which was ascribed to the inclusion of fluorine on the *ortho*-

**Table 2.** Optical and Electrochemical Properties of Polymers.

polymer	Solution			Film		$E_g^{opt}$ [eV] <sup>b</sup>	HOMO [eV] <sup>c</sup>	LUMO [eV] <sup>d</sup>	HOMO [eV] <sup>e</sup>	LUMO [eV] <sup>f</sup>
	$\lambda_{max}$ [nm]	$\lambda_{shoulder}$ [nm]	$\lambda_{max-H^a}$ [nm]	$\lambda_{max}$ [nm]	$\lambda_{edge}$ [nm]					
P1	560	645	545	603	708	1.75	-5.50	-3.75	-5.03	-3.28
P2	544	N/A	543	589	683	1.82	-5.63	-3.81	-5.49	-3.67
P3	555	623	542	586	686	1.81	-5.56	-3.75	-5.13	-3.32

<sup>a</sup> The data were obtained in chlorobenzene solution at high temperature. <sup>b</sup> Band gap was calculated from the onset of the film absorption. <sup>c</sup> Measured by cyclic voltammetry (CV). <sup>d</sup> Calculated from the gap of  $E_g^{opt}$  and HOMO values obtained from CV data. <sup>e</sup> Measured by ultraviolet photoelectron spectroscopy (UPS). <sup>f</sup> Calculated from the gap of  $E_g^{opt}$  and HOMO values obtained from UPS spectra.

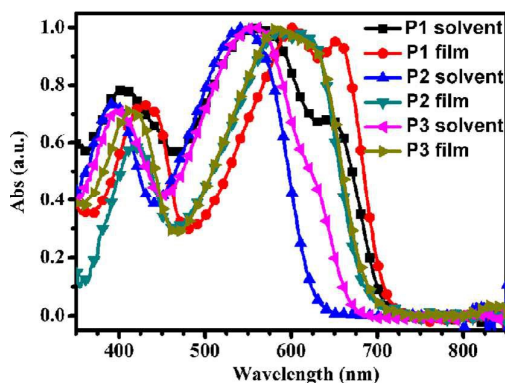


**Figure 3.** Normalized UV-vis absorption spectra of P1, P2, P3 in chlorobenzene solution and in the thin solid film at 25 °C. position of the phenyl substituted BDT. Therefore, high  $V_{oc}$  for the devices based on P2 and P3 would be expected<sup>35</sup>. As a verification of the CV results, UPS spectra of the three polymers were also provided in Figure S2. A similar changing trend for the HOMO of the three polymers was observed from the UPS results (Table 2), which indicated that the comparison of HOMO energy levels among the polymers was reliable in this work. To further understand the above experimental results, the calculations of energies and distributions of the frontier molecular orbitals of these polymers were performed by density functional theory (DFT) using the Gaussian 09 program at the B3LYP/6-31G(d,p) level in the gas phase<sup>36</sup>. The optimized molecular geometries were confirmed to be minimum-energy conformations since there were no imaginary frequencies by vibrational calculation at the same level. In this work, only one repeating unit was chosen, and alkyl chains on the alkoxyphenyl substituted group and DTBTff unit were simplified to methyl group to reduce the calculation time. The fluorine atom substituted on BDTP was put adjacent to the hydrogen atom on the backbone of BDT unit (see the conformation 2 in Figure S3a) to avoid the repulsive force of the hydrogen atom, which would increase the calculated total energy. Figure S3b showed the molecular geometries and electronic wave function distribution of the HOMO and LUMO of the D- $\pi$ -A model compounds. For the three polymers, the electronic wave function of the HOMO was distributed entirely over the conjugated molecule, which was beneficial for obtaining higher hole mobility<sup>25</sup>. The electronic wave function of the LUMO was mainly localized on the electron accepting

segment. The calculated HOMO and LUMO energy levels of P1, P2, P3 were quantitatively in agreement with the observed experimental results, which confirmed that the fluorine substituted on the *ortho*-position of the alkoxyphenyl side groups would lower the HOMO energy level efficiently.

The normalized UV-visible absorption spectra of three polymers P1, P2, and P3 in chlorobenzene solution and thin films at 25 °C are shown in Figure 3. The spectra of the three polymers in the chlorobenzene solution under different temperature are also presented in Figure S4. The absorption data were summarized in Table 2. As shown in Figure 3, these polymers showed quite different absorption bands in chlorobenzene solution with major absorption peaks at 560 nm for P1, 544 nm for P2, and 555 nm for P3, which were assigned to the intra-molecular charge transfer (ICT)<sup>37</sup>. Meanwhile, a strong shoulder peak at around 645 nm for P1, and a weak one at around 623 nm for P3 were observed, which indicated the different aggregation ability of the two polymers in solution<sup>38</sup>. Interestingly, no shoulder peak for P2 in solution was found, which indicated that the aggregation ability of P2 was much weaker than those of P1 and P3. With increasing the temperature, the intensities of the shoulder peaks of P1 and P3 were declined gradually (Figure S4a and S4c), because the aggregations of the polymers were weakened step by step. Finally, the shoulder peaks were disappeared and all the three polymers exhibited similar absorption profiles (Table 2, and Figure S4), while the aggregations of the polymers in solutions were all broken at high temperature. The above results indicated that the different absorption spectra in solution at room temperature were mainly caused by the different aggregation ability of the three polymers, which originated from the different substituted groups or side chains. Compared to P1, the inclusion of the fluorine on the *ortho*-position of the BDTP moiety could enlarge the dihedral angle  $\theta_1$  (Table S2) between the conjugated side chains and backbone of the polymer. Furthermore, the electron density of conjugated backbone was reduced because of the electron-withdrawing ability of the fluorine on the *ortho*-position<sup>21</sup>, which could further weaken the  $\pi$ -orbital overlap between BDT and adjacent thiophene rings in DTBTff moiety<sup>21, 39-41</sup>, and thus enlarge the dihedral angle  $\theta_3$ <sup>29, 42</sup>. Therefore, the inclusion of fluorine on the *ortho*-position of BDTP can significantly tune the conformation and

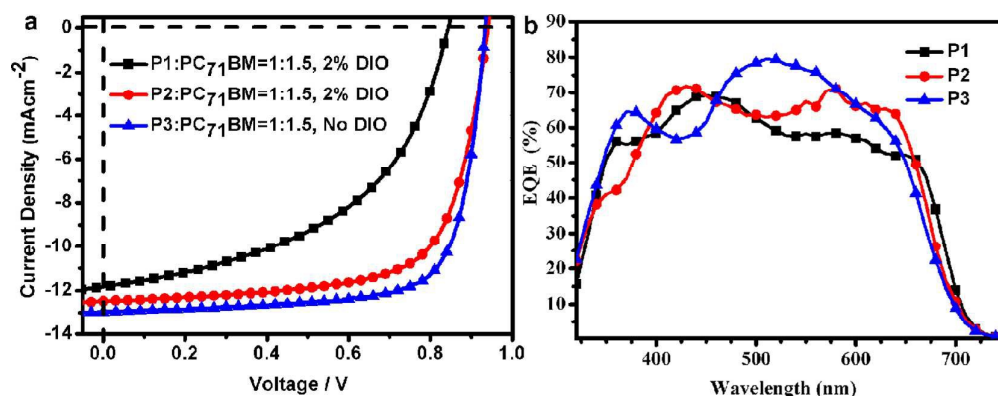


Figure 4. (a) Optimized  $J$ - $V$  curves of PSCs based on the polymer/ $PC_{71}BM$  blend film. (b) EQE spectra of the optimized devices.

Table 3. Optimized photovoltaic performance of polymers

polymer	Ratio <sup>a</sup> /Additive	$V_{oc}$ (V)	$J_{sc}$ (mA cm <sup>-2</sup> )	FF (%)	PCE <sub>max</sub> (PCE <sub>ave</sub> ) <sup>b</sup> (%)
P1	1:1.5/2% DIO	0.84	11.81	49.43	4.91 (4.72)
P2	1:1.5/2% DIO	0.94	12.48	69.03	8.10 (8.05)
P3	1:1.5/No additive	0.93	12.97	74.49	9.02 (8.96)

<sup>a</sup>The weight ratio of polymer to  $PC_{71}BM$ ; <sup>b</sup>The average PCE is obtained from 20 devices.

aggregation of P2. On the other hand, the dihedral angle  $\theta_3$  in P3 was very small, probably due to the smaller steric hindrance of the linear hexyl in P3 than the branched 2-ethyl-hexyl side chain in P2<sup>32</sup>, indicating that the aggregation and planarity of P3 could be strengthened in some extent compared to P2. As discussed above, the incorporation of fluorine on the ortho position of alkoxyphenyl substituted BDT unit will weaken the aggregation of its resultant polymer (from P1 to P2), and the substitute of 2-ethyl-hexyl side chains with hexyl group on the thiophene bridge will strengthen the aggregation of the relevant polymer (from P2 to P3). It is clear that the above two effects on the aggregation is opposite. In our designed polymer system, the effect of former (introducing fluorine) is more effective than that of the later one (changing the alkyl side chains). As a result, P3 is more aggregated than P2.

In the solid state, the main absorption profiles become broader, and the maximum absorption peaks moved toward longer wavelength to 603 nm for P1, 589 nm for P2, and 586 nm for P3, respectively. These large red-shifts against the absorption in solution meant stronger interchain  $\pi$ - $\pi$  stacking in the solid state. The optical band gaps were estimated as 1.75, 1.82, and 1.81 eV for P1, P2, and P3, respectively, from the onsets of the UV-vis absorption in the thin solid films.

### 2.3. Polymer Solar Cell Performance

Photovoltaic properties of polymers were investigated with a device structure of ITO/PEDOT:PSS/Polymer: $PC_{71}BM$ /Ca/Al under the illumination of AM 1.5G at 100 mA cm<sup>-2</sup>. The device fabrication conditions, such as the weight ratio of polymer to  $PC_{71}BM$ , and the amount of the 1,8-diiodooctane (DIO) additive were carefully optimized. As shown in Figure S5 and Table 3, the optimal D/A ratios for P1, P2 and P3 were all 1:1.5. The device of P1: $PC_{71}BM$  at 1:1.5 weight ratio showed a  $V_{oc}$  of 0.88 V, a  $J_{sc}$  of 11.27 mA/cm<sup>2</sup>, a FF of 46.96%, and correspondingly a PCE of 4.67% (Table S3). At the

same ratio, a  $V_{oc}$  of 1.03 V was obtained for P2, which was 0.15 V higher than that of P1. Obviously, the higher  $V_{oc}$  of P2 based device resulted from the deeper HOMO energy level of P2. Then, 1,8-diiodooctane (DIO) was used as the additive to further optimize the morphology of the above polymer/ $PC_{71}BM$  blends with volume fraction of 1, 2, and 3%. Unfortunately, only a small improvement of P1-device performance was observed. The optimized amount of DIO was 2% and the device showed a PCE of 4.91% with a  $V_{oc}$  of 0.84 V, a  $J_{sc}$  of 11.81 mA/cm<sup>2</sup>, a FF of 49.43%. However, DIO has significant effect on the P2/ $PC_{71}BM$  blend. When 2% DIO was added, a  $J_{sc}$  of 12.48 mA cm<sup>-2</sup> was obtained, and the FF improved to 69.03%, a higher PCE of 8.10% was realized (Table 3). It should be noted that the  $V_{oc}$  of 0.94 V for the optimized P2/ $PC_{71}BM$  device was one of the highest values derived from the polymers with PBBDT-DTBTff backbone<sup>16, 17</sup>. Excitingly, without any processing additives or post-treatments, the devices based on P3 exhibited a maximum PCE of 9.02%, with a  $V_{oc}$  of 0.93 V, a  $J_{sc}$  of 12.97 mA/cm<sup>2</sup>, and a FF of 74.49%, which was the first reported single junction device with PCE over 9% based on BDT-DTBTff structure, meanwhile, it was also the highest one for the D-A polymers with fluorine substituted BDT as electron-donor units in single junction polymer solar cells. The performance of P3 based devices showed no improvement when treated with DIO (Table S3).

The EQE spectra of P3 gave the photo-to-current response in the wavelength range from 330-700 nm with maximum 79% at 515 nm, as shown in Figure 4b, illustrating the high  $J_{sc}$  of the P3-device obtained. The substantial EQE together with a high fill factor of 74.49% for the P3 device, probably reflected higher hole mobility and more preferable morphology of active-layer for the P3-device compared to those of P1 and P2<sup>43</sup>. The  $J_{sc}$  values (11.35 mA cm<sup>-2</sup> for P1, 12.02 mA cm<sup>-2</sup> for P2 and 12.37 mA cm<sup>-2</sup> for P3) integrated from the EQE spectra were consistent well with the  $J_{sc}$  recorded from the  $J$ - $V$  measurements.

### 2.4. Morphological Characterization of the Active Layer

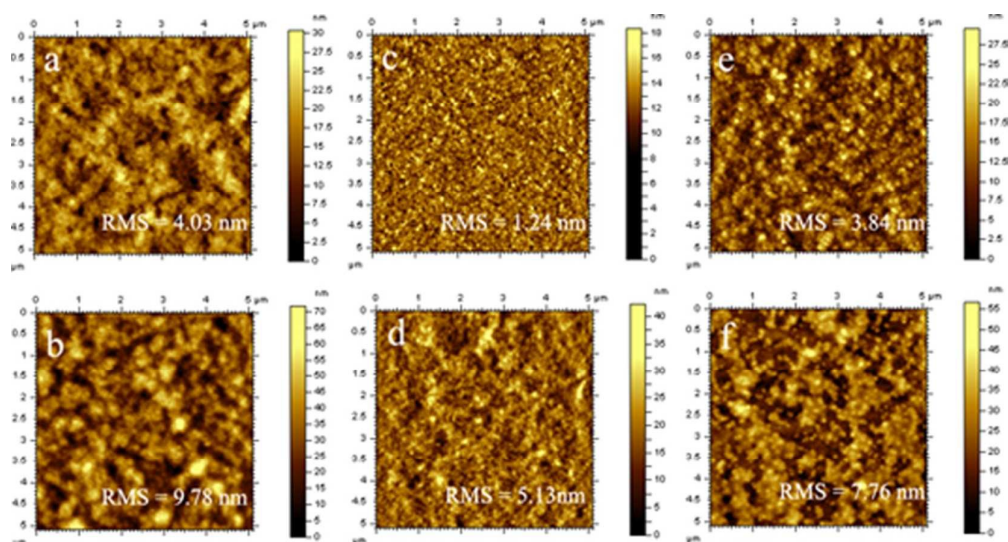


**Figure 5.** AFM height images of the active layers of P1/PC<sub>71</sub>BM (a), P1/PC<sub>71</sub>BM with 2% DIO (b), P2/PC<sub>71</sub>BM (c), P2/PC<sub>71</sub>BM with 2% DIO (d), P3/PC<sub>71</sub>BM (e), and P3/PC<sub>71</sub>BM with 2% DIO (f).

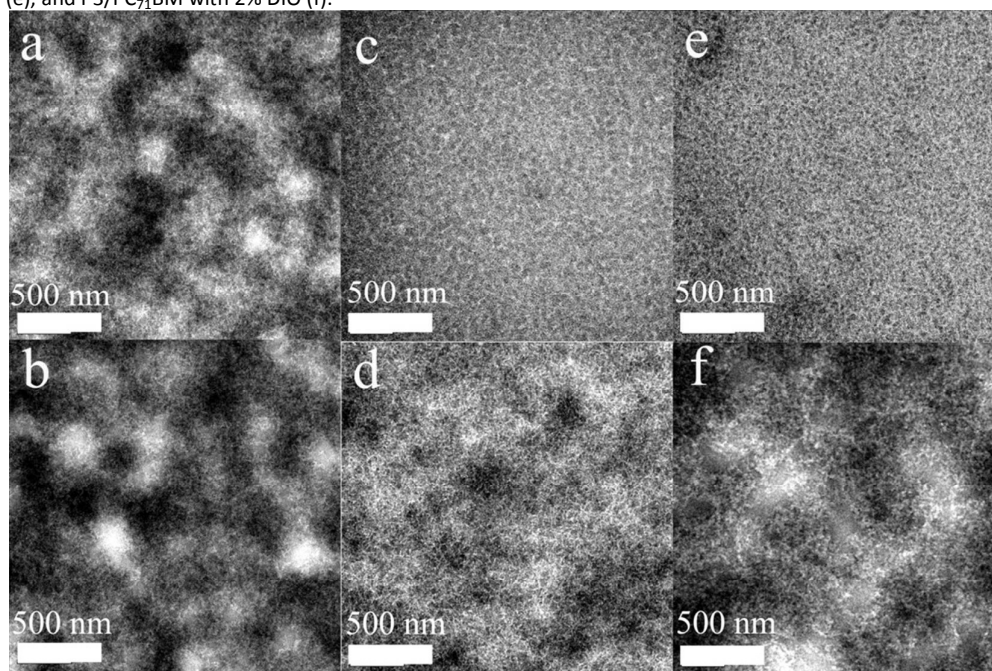


**Figure 6.** TEM images of the active layers of P1/PC<sub>71</sub>BM (a), P1/PC<sub>71</sub>BM with 2% DIO (b), P2/PC<sub>71</sub>BM (c), P2/PC<sub>71</sub>BM with 2% DIO (d), P3/PC<sub>71</sub>BM (e), and P3/PC<sub>71</sub>BM with 2% DIO (f).

The morphologies of the blend films of polymers and PC<sub>71</sub>BM have been examined by tapping-mode atomic force microscopy (AFM) and transmission electron microscope (TEM). All the blend films were prepared under the same conditions with the optimized photovoltaic devices. As shown in Figure 5a, the blend film of P1 and PC<sub>71</sub>BM showed a surface root mean square (RMS) roughness (4.03 nm). While the blend film was spin-coated from *o*-

dichlorobenzene solution containing 2.0% DIO as additive, the RMS data increased to 9.78 nm (Figure 5b). Meanwhile, its TEM image showed large polymer and PC<sub>71</sub>BM aggregation domains (Figure 6b), which indicated poor phase separation in the blend film. This might be one of the reasons for the much lower FF (49.43%) for the P1 based device.<sup>44</sup> Compared to P1, the only difference in chemical structure of P2 is the introduction of the fluorine on the

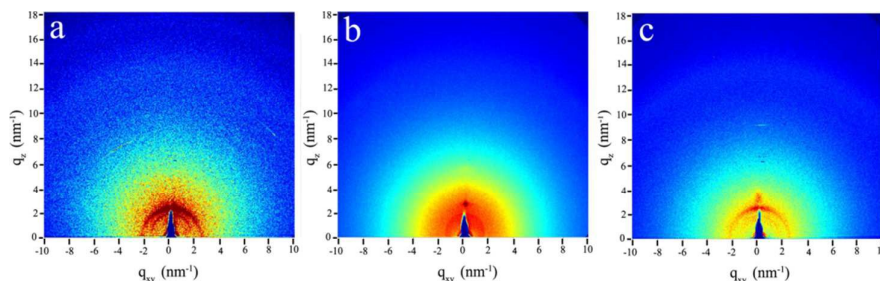


**Figure 7.** 2D GIWAXS images of the polymer:PC<sub>71</sub>BM blend films processed under optimized device fabrication conditions, P1/PC<sub>71</sub>BM (1:1.5) with 2% DIO treatment (a); P2/PC<sub>71</sub>BM (1:1.5) with 2% DIO treatment (b); P3/PC<sub>71</sub>BM (1:1.5) without DIO treatment (c).

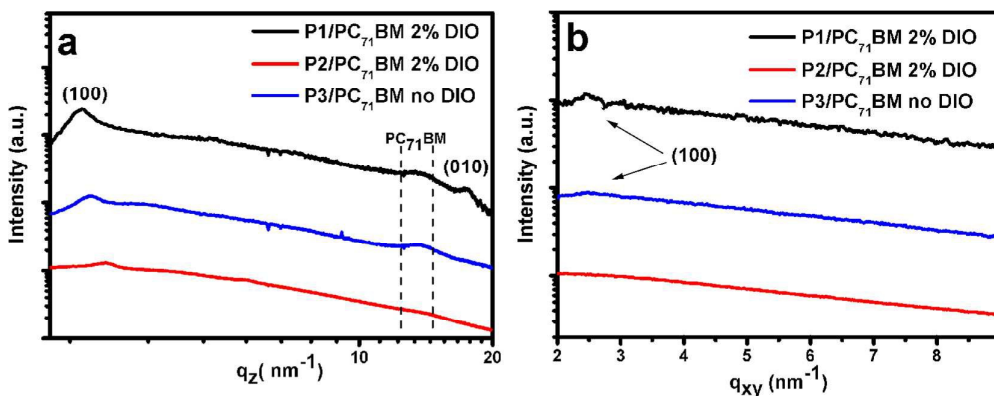


**Figure 8.** Linecuts of 2D GIWAXS images of the polymer:PC<sub>71</sub>BM blend films under optimized device fabrication conditions.

*ortho*-position of BDTP. However, a quite different morphology was observed for the blend film of P2 and PC<sub>71</sub>BM. A very smooth surface with a small RMS roughness (1.24 nm) was found. The TEM image of the blend film also showed a well-ordered separation network distribution between polymer and acceptor (Figure 6c). While the blend films were spin-coated from *o*-dichlorobenzene solution containing 2.0% DIO as additive, the RMS data was increased to 5.13 nm. The morphology change of the active layer after treated with DIO, which would result in different contact situation between the donor and acceptor domains, might be one of the possible reasons for the decrease of  $V_{oc}$  value for the P2-based devices with DIO additive treatment.<sup>45-47</sup> As shown in Figure 6d, a fibrillar-like bicontinuous interpenetrating network were observed. This might explain the higher FF of 69.03% for the P2 based devices.<sup>48</sup> These results indicated that the inclusion of fluorine on the *ortho*-position of BDTP segment in P2 could efficiently tune the aggregation of the polymer and improve the miscibility of the polymer with PC<sub>71</sub>BM in the blend films. Polymers P2 and P3 shared the same conjugating backbone, the only difference was the nonchromophoric alkyl chains in the thiophene bridge in the BDT-DTBTff backbone. However, the influence of the DIO on the morphology of the blend film was quite different. Without treatment by DIO, the neat blend film of P3 with PC<sub>71</sub>BM showed a uniform interpenetrating structure with a RMS data of 3.84 nm (Figure 5e and 6e), while 2% DIO was added, large P3 and PC<sub>71</sub>BM domains appeared and the RMS data of the film increased to 7.76 nm, which might account for the decline of FF to 57.61%.<sup>49</sup>

The above results indicated that the morphology of the active layer could be optimized by precise modification of the chemical structure of polymer. In our work, P1 had the strongest self-aggregation ability, which resulted in the large phase separation of P1/PC<sub>71</sub>BM blend film. It was also consistent with their optical properties. After introduction fluorine on the *ortho*-position of BDTP segment, the aggregation ability of P2 was weakened drastically, which made it form a preferable blend film with PC<sub>71</sub>BM after DIO treatment. To further decrease the steric hindrance and improve the planarity, branched 2-ethylhexyl group was replaced with linear hexyl group in P3. As a result, the blend film of P3 and PC<sub>71</sub>BM showed a well ordered nanoscale phase separation without DIO treatment. It can be seen from our results that the morphology of the active layer can be optimized from the following two methods. One is using post-treatment technique such as adding additive, which can tune the morphology and phase separation of the active layer in the process of film formation. In this work, the performance of P2 is optimized through this way. The other pathway is to optimize the chemical structures of the polymers, which can affect on the conformation and aggregation of the polymers. In this work, the molecular structure of P3 with suitable side chain can make the active layer exhibit preferable morphology, and finally show champion performance without additive.

## 2.5. Hole Mobility and Crystalline Structures

To further analyze and understand the photovoltaic performance of the PSCs, the hole mobility was measured using a vertical diode with the device structure of ITO/PEDOT:PSS/polymer:PC<sub>71</sub>BM/Au and the *J-V* curves were shown in Fig. S6. By taking current-voltage in the range of 0-4 V and fitting the results to a space charge limited current (SCLC) model, where the SCLC is described by  $J_{\text{SCLC}} = (9/8) \epsilon_0 \epsilon_r \mu_h (V^2)/(L^3)$ , where *J* stands for current density,  $\epsilon_0$  is the permittivity of free space,  $\epsilon_r$  is the relative dielectric constant of the transport medium,  $\mu_h$  is the hole mobility, *V* is the internal potential in the device and *L* is the thickness of the active layer, the hole mobilities for P1, P2, and P3 are calculated to be  $1.7 \times 10^{-5} \text{ cm}^2 \text{ V}^{-1} \text{ s}^{-1}$ ,  $5.7 \times 10^{-5} \text{ cm}^2 \text{ V}^{-1} \text{ s}^{-1}$ , and  $1.5 \times 10^{-4} \text{ cm}^2 \text{ V}^{-1} \text{ s}^{-1}$ , respectively. Among the three polymers, P3 exhibits the highest hole mobility, which is 2.6 times and 8.8 times larger than those of P2 and P1, respectively. The higher mobility contributes to obtaining high  $J_{\text{sc}}$  and FF of the P3 based devices.

Grazing incidence wide-angle X-ray scattering (GIWAXS) method was used to further characterize the crystalline structure of the active layer of the PSCs. In our experiment, all the blend films were prepared on the silicon substrates following the same fabrication conditions as used for the optimized photovoltaic devices. As shown in Figure 7a and Figure 8, the (100) diffraction peak in the out-of-plane pattern at  $q_z = 2.34 \text{ nm}^{-1}$  was observed for the blend film of P1 and PC<sub>71</sub>BM with 2% DIO treatment, indicating an edge-on alignment of P1 with a lamellar distance of 2.69 nm. In addition, a weak (010) peak ( $q_z = 17.5 \text{ nm}^{-1}$ , d-spacing = 0.36 nm) also appeared in the out-of-plane direction, indicating some face-on crystallites existed<sup>50</sup>. Although crystalline structure was found in the active layer of optimized P1-devices, the excessively strong self-aggregating ability of P1 and large phase separation in the blend film might hinder the formation of interpenetrating bicontinuous networks of P1 and PC<sub>71</sub>BM, which would increase geminate recombination at the interface of the donor and acceptor domains, and result in poor mobility and device performance of P1 based devices<sup>51-53</sup>. As for the blend films containing P2 or P3, polymer crystallinity was observed to be relatively low due to the much lower (100) peak intensity and the absolutely absence of any other higher order reflections<sup>54, 55</sup>. Nevertheless, P3/PC<sub>71</sub>BM blend film showed a broad (100) peak in the in-plane direction, indicating the existence of some crystalline structure in the face-on pattern, which may be one of the possible reasons for the higher device performance of P3 than that of P2<sup>56</sup>.

### 3. Conclusion

In conclusion, fluorine atom was firstly introduced to the *ortho*-position of alkoxyphenyl group on BDT units. Subsequently, three polymers, named PBDTP-DTBTff (P1), P-*o*-FBDTP-C8DTBTff (P2) and P-*o*-FBDTP-C6DTBTff (P3), were constructed. The optical properties, molecular energy levels, hole mobility, morphology and crystalline structures of the three polymers showed significant difference, which resulted in obviously different device performance. Finally, the optimized device of P3 demonstrated a PCE of 9.02% without any additive

treatment, which was 11.4% and 83.7% higher than those of P2 and P1, respectively. Note that the PCE of 9.02% is the highest value for the reported D-A polymers with BDT-DTBTff as backbone in single junction polymer solar cells. Our work indicates that a BDT unit with fluorine on the *ortho*-position of alkoxyphenyl side chains is a promising electron-donor building block for highly efficient light-harvesting polymers, and there is still room for further improvement of the device performance through rational selecting the electron-acceptor segment and alkyl side chains on the D-A conjugated polymers.

### Acknowledgements

This work was supported by the National Natural Science Foundation of China (21204097, 21274161, 51173199, 51573205, and 61405209), the Ministry of Science and Technology of China (2014CB643501, 2010DFA52310), and Qingdao Municipal Science and Technology Program (14-2-4-28-jch). The authors thank beamline BL16B1 (Shanghai Synchrotron Radiation Facility) for providing the beam time. N. Wang and W. Chen contributed equally to this work.

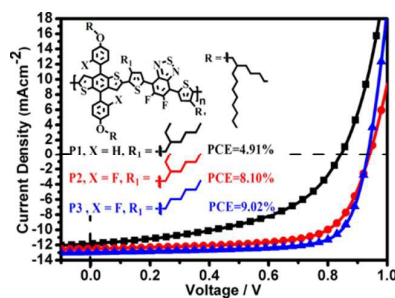
### Notes and references

- 1 Y. Li, *Acc. Chem. Res.* 2012, **45**, 723-733.
- 2 W. Zhang, B. Zhao, Z. He, X. Zhao, H. Wang, S. Yang, H. Wu, Y. Cao, *Energy Environ. Sci.* 2013, **6**, 1956-1964.
- 3 C. Duan, W. Cai, B. B. Y. Hsu, C. Zhong, K. Zhang, C. Liu, Z. Hu, F. Huang, G. C. Bazan, A. J. Heeger, Y. Cao, *Energy Environ. Sci.* 2013, **6**, 3022-3034.
- 4 L. M. Chen, Z. R. Hong, G. Li, Y. Yang, *Adv. Mater.* 2009, **21**, 1434-1449.
- 5 C. C. Chueh, C. Z. Li, A. K. Y. Jen, *Energy Environ. Sci.* 2015, **8**, 1160-1189.
- 6 G. Li, R. Zhu, Y. Yang, *Nat. Photon.* 2012, **6**, 153-161.
- 7 Y. Liu, J. Zhao, Z. Li, C. Mu, W. Ma, H. Hu, K. Jiang, H. Lin, H. Ade, H. Yan, *Nat. Commun.* 2014, **5**, 5293.
- 8 Z. C. He, B. Xiao, F. Liu, H. B. Wu, Y. L. Yang, S. Xiao, C. Wang, T. P. Russell, Y. Cao, *Nat. Photon.* 2015, **9**, 174-179.
- 9 D. Gendron, M. Leclerc, *Energy Environ. Sci.* 2011, **4**, 1225-1237.
- 10 X. Guo, S. R. Puniredd, M. Baumgarten, W. Pisula, K. Mullen, *J. Am. Chem. Soc.* 2012, **134**, 8404-8407.
- 11 H. Kim do, B. L. Lee, H. Moon, H. M. Kang, E. J. Jeong, J. I. Park, K. M. Han, S. Lee, B. W. Yoo, B. W. Koo, J. Y. Kim, W. H. Lee, K. Cho, H. A. Becerril, Z. Bao, *J. Am. Chem. Soc.* 2009, **131**, 6124-6132.
- 12 S. Y. Ku, M. A. Brady, N. D. Treat, J. E. Cochran, M. J. Robb, E. J. Kramer, M. L. Chabinyc, C. J. Hawker, *J. Am. Chem. Soc.* 2012, **134**, 16040-16046.
- 13 J. Lee, J. H. Kim, B. Moon, H. G. Kim, M. Kim, J. Shin, H. Hwang, K. Cho, *Macromolecules* 2015, **48**, 1723-1735.
- 14 J. Hou, M.-H. Park, S. Zhang, Y. Yao, L.-M. Chen, J.-H. Li, Y. Yang, *Macromolecules* 2008, **41**, 6012-6018.
- 15 W. C. Huang, E. Gann, L. Thomsen, C. K. Dong, Y. B. Cheng, C. R. McNeill, *Adv. Energy Mater.* 2015, **5**, 1401259.
- 16 J.-H. Kim, C. E. Song, B. Kim, I.-N. Kang, W. S. Shin, D.-H. Hwang, *Chem. Mater.* 2014, **26**, 1234-1242.
- 17 J. X. Wang, M. J. Xiao, W. C. Chen, M. Qiu, Z. K. Du, W. G. Zhu, S. G. Wen, N. Wang, R. Q. Yang, *Macromolecules* 2014, **47**, 7823-7830.
- 18 D. Y. Liu, C. Y. Gu, M. J. Xiao, M. Qiu, M. L. Sun, R. Q. Yang, *Polym. Chem.* 2015, **6**, 3398-3406.

## ARTICLE

## Journal Name

- 19 W. H. Tseng, H. C. Chen, Y. C. Chien, C. C. Liu, Y. K. Peng, Y. S. Wu, J. H. Chang, S. H. Liu, S. W. Chou, C. L. Liu, Y. H. Chen, C. I. Wu, P. T. Chou, *J. Mater. Chem. A* 2014, **2**, 20203-20212.
- 20 H. Zhou, L. Yang, A. C. Stuart, S. C. Price, S. Liu, W. You, *Angew. Chem. Int. Ed.* 2011, **50**, 2995-2998.
- 21 H. J. Son, W. Wang, T. Xu, Y. Liang, Y. Wu, G. Li, L. Yu, *J. Am. Chem. Soc.* 2011, **133**, 1885-1894.
- 22 D. L. Liu, W. C. Zhao, S. Q. Zhang, L. Ye, Z. Zheng, Y. Cui, Y. Chen, J. H. Hou, *Macromolecules* 2015, **48**, 5172-5178.
- 23 M. Zhang, X. Guo, S. Zhang, J. Hou, *Adv. Mater.* 2014, **26**, 1118-1123.
- 24 W. Chen, Z. Du, L. Han, M. Xiao, W. Shen, T. Wang, Y. Zhou, R. Yang, *J. Mater. Chem. A* 2015, **3**, 3130-3135.
- 25 J. Yuan, Y. Zou, R. Cui, Y.-H. Chao, Z. Wang, M. Ma, Y. He, Y. Li, A. Rindgen, W. Ma, D. Xiao, Z. Bo, X. Xu, L. Li, C.-S. Hsu, *Macromolecules* 2015, **48**, 4347-4356.
- 26 G. Li, X. Gong, J. Zhang, Y. Liu, S. Feng, C. Li, Z. Bo, *ACS Appl. Mater. Interfaces*, DOI: 10.1021/acsami.5b08769
- 27 B. Qiu, J. Yuan, X. Xiao, D. He, L. Qiu, Y. Zou, Z. G. Zhang, Y. Li, *ACS Appl. Mater. Interfaces* 2015, **7**, 25237-25246.
- 28 N. Chakravarthi, K. Gunasekar, K. Kranthiraja, T. Kim, W. Cho, C. S. Kim, D. H. Kim, M. Song, S. H. Jin, *Polym. Chem.* 2015, **6**, 7149-7159.
- 29 L. L. Han, W. C. Chen, T. Hu, J. Z. Ren, M. Qiu, Y. H. Zhou, D. Q. Zhu, N. Wang, M. L. Sun, R. Q. Yang, *ACS Macro. Letters* 2015, **4**, 361-366.
- 30 J. Yuan, L. Xiao, B. Liu, Y. Li, Y. He, C. Pan, Y. Zou, *J. Mater. Chem. A* 2013, **1**, 10639-10645.
- 31 G. L. Grunewald, A. J. Kolar, M. S. S. Palanki, V. M. Paradkar, T. J. Reitz, D. J. Sall, *Org. Prep. Proced. Int.* 1990, **22**, 747-753.
- 32 N. Wang, Z. Chen, W. Wei, Z. Jiang, *J. Am. Chem. Soc.* 2013, **135**, 17060-17068.
- 33 C. P. Yau, S. Wang, N. D. Treat, Z. P. Fei, B. J. T. de Villers, M. L. Chabiny, M. Heeney, *Adv. Energy Mater.* 2015, **5**, 1401228
- 34 N. Wang, X. C. Bao, Y. Yan, D. Ouyang, M. L. Sun, V. A. L. Roy, C. S. Lee, R. Q. Yang, *J. Polym. Sci., Part A: Polym. Chem.* 2014, **52**, 3198-3204.
- 35 Z. Ma, W. Sun, S. Himmelberger, K. Vandewal, Z. Tang, J. Bergqvist, A. Salleo, J. W. Andreasen, O. Inganas, M. R. Andersson, C. Muller, F. Zhang, E. Wang, *Energy Environ. Sci.* 2014, **7**, 361-369.
- 36 M. J. Frisch, G. W. Trucks, H. B. Schlegel, G. E. Scuseria, M. A. Robb, J. R. Cheeseman, G. Scalmani, V. Barone, B. Mennucci, G. A. Petersson, H. Nakatsuji, M. Caricato, X. Li, H. P. Hratchian, A. F. Izmaylov, J. Bloino, G. Zheng, J. L. Sonnenberg, M. Hada, M. Ehara, K. Toyota, R. Fukuda, J. Hasegawa, M. Ishida, T. Nakajima, Y. Honda, O. Kitao, H. Nakai, T. Vreven, J. A. Montgomery, J. E. Peralta Jr., F. Ogliaro, M. Bearpark, J. J. Heyd, E. Brothers, K. N. Kudin, V. N. Staroverov, T. Keith, R. Kobayashi, J. Normand, K. Raghavachari, A. Rendell, J. C. Burant, S. S. Iyengar, J. Tomasi, M. Cossi, N. Rega, J. M. Millam, M. Klene, J. E. Knox, J. B. Cross, V. Bakken, C. Adamo, J. Jaramillo, R. Gomperts, R. E. Stratmann, O. Yazyev, A. J. Austin, R. Cammi, C. Pomelli, J. W. Ochterski, R. L. Martin, K. Morokuma, V. G. Zakrzewski, G. A. Voth, P. Salvador, J. J. Dannenberg, S. Dapprich, A. D. Daniels, O. Farkas, J. B. Foresman, J. V. Ortiz, J. Cioslowski, D. J. Fox, *Gaussian 09, Revision A.1*, Gaussian, Inc., Wallingford, CT 2009.
- 37 D. Ouyang, M. J. Xiao, D. Q. Zhu, W. G. Zhu, Z. K. Du, N. Wang, Y. H. Zhou, X. C. Bao, R. Q. Yang, *Polym. Chem.* 2015, **6**, 55-63.
- 38 D. P. Qian, L. Ye, M. J. Zhang, Y. R. Liang, L. J. Li, Y. Huang, X. Guo, S. Q. Zhang, Z. A. Tan, J. H. Hou, *Macromolecules* 2012, **45**, 9611-9617.
- 39 J. Min, Z. G. Zhang, S. Y. Zhang, Y. F. Li, *Chem. Mater.* 2012, **24**, 3247-3254.
- 40 S. Wood, J. H. Kim, D. H. Hwang, J. S. Kim, *Chem. Mater.* 2015, **27**, 4196-4204.
- 41 P. Shen, H. J. Bin, L. Xiao, Y. F. Li, *Macromolecules* 2013, **46**, 9575-9586.
- 42 M. R. Andersson, M. Berggren, O. Inganäs, G. Gustafsson, J. C. Gustafsson-Carlberg, D. Selse, T. Hjertberg, O. Wennerström, *Macromolecules* 1995, **28**, 7525-7529.
- 43 M. Helgesen, J. E. Carle, F. C. Krebs, *Adv. Energy Mater.* 2013, **3**, 1664-1669.
- 44 S. H. Park, A. Roy, S. Beaupre, S. Cho, N. Coates, J. S. Moon, D. Moses, M. Leclerc, K. Lee, A. J. Heeger, *Nat. Photon.* 2009, **3**, 297-302.
- 45 C. Gu, Q. Zhu, X. Bao, S. Wen, M. Qiu, L. Han, W. Huang, D. Zhu, R. Yang, *Polym. Chem.* 2015, **6**, 6219-6226.
- 46 Y. Sun, J. Seifert, M. Wang, L. A. Perez, C. Luo, G. C. Bazan, F. Huang, Y. Cao, A. J. Heeger, *Adv. Energy Mater.* 2014, **4**, 1301601.
- 47 Y. Li, Y. Yang, X. Bao, M. Qiu, Z. Liu, N. Wang, G. Zhang, R. Yang, D. Zhang, *J. Mater. Chem. C* 2016, **4**, 185-192.
- 48 W. Li, K. H. Hendriks, A. Furlan, W. S. Roelofs, M. M. Wienk, R. A. Janssen, *J. Am. Chem. Soc.* 2013, **135**, 18942-18948.
- 49 S. Engmann, C. R. Singh, V. Turkovic, H. Hoppe, G. Gobsch, *Adv. Energy Mater.* 2013, **3**, 1463-1472.
- 50 L. W. Wang, D. Ma, S. W. Shi, S. Chen, Y. F. Li, X. Y. Li, H. Q. Wang, *J. Mater. Chem. A* 2015, **3**, 21460-21470.
- 51 H. Cha, H. N. Kim, T. K. An, M. S. Kang, S.-K. Kwon, Y.-H. Kim, C. E. Park, *ACS Appl. Mater. Interfaces* 2014, **6**, 15774-15782.
- 52 W. Lee, H. Cha, Y. J. Kim, J.-E. Jeong, S. Hwang, C. E. Park, H. Y. Woo, *ACS Appl. Mater. Interfaces* 2014, **6**, 20510-20518.
- 53 D. Credgington, R. Hamilton, P. Atienzar, J. Nelson, J. R. Durrant, *Adv. Funct. Mater.* 2011, **21**, 2744-2753.
- 54 X. Guo, M. Zhang, W. Ma, L. Ye, S. Zhang, S. Liu, H. Ade, F. Huang, J. Hou, *Adv. Mater.* 2014, **26**, 4043-4049.
- 55 J. R. Tumbleston, A. C. Stuart, E. Gann, W. You, H. Ade, *Adv. Funct. Mater.* 2013, **23**, 3463-3470.
- 56 M. Zhang, Y. Gu, X. Guo, F. Liu, S. Zhang, L. Huo, T. P. Russell, J. Hou, *Adv. Mater.* 2013, **25**, 4944-4949.



The polymer, with *o*-fluoro-*p*-alkoxyphenyl- substituted benzo[1,2-b:4,5-b']dithiophene units as electron-rich segment and 5,6-difluoro-4,7-di(4-hexyl-2-thienyl)-2,1,3-benzothiadiazole as electron-withdrawing unit, shows a PCE of 9.02%.